

Free surface integrals in non-linear wave-diffraction analysis

J. B. Huang¹, R. Eatock Taylor¹ and R. C. T. Rainey²

¹*Department of Engineering Science, University of Oxford, U. K.*

²*W. S. Atkins Consultants Ltd, Epsom, Surrey, U. K.*

A difficult problem in frequency-domain analysis of non-linear wave interaction with offshore structures is the evaluation of the two-dimensional free-surface integral, which provides the 'locked wave' component of the diffraction potential. This is usually done by meshing the free-surface of the fluid domain into boundary elements, and carrying out the integration element-by-element. The approach is known to be very time-consuming, especially if needed for computing the third-order forces, where it is necessary to evaluate the second-order potentials over a large domain on the free-surface. This paper proposes an alternative way of performing the free-surface integrations. We first extend the integration domain into the entire free-surface, then subtract out the contribution from the internal water plane occupied by the structures. In this way an efficient semi-analytical method can be developed, and the integrals are reduced to one-dimensional quadratures. The algorithm presented in the paper is relevant to obtaining the 'locked wave' component of the diffraction potential at either second or third order.

1. Semi-analytical method for the free surface integrals

We consider the locked wave component of the potential associated with diffraction by an array of vertical, surface-piercing structures of arbitrary shape. We define a global co-ordinate system (x, y, z) and a number of local cylindrical co-ordinate systems (r_k, θ_k, z) which coincide with the individual structures. The z axis originates from the quiescent free-surface and points upwards. For simplicity we only consider the second-order potential, but the formulation is also valid at third order. In the local coordinate system, the locked wave potential can be expressed as:

$$\phi_p^{(2)}(r_k, \theta_k, z) = \int \int_{S_f} Q^{(2)}(s) G^{(2)}(r_k, \theta_k, z; s) ds \quad (1)$$

where S_f is the entire free-surface of the fluid domain, $Q^{(2)}$ is the forcing function and $G^{(2)}$ the Green function.

We rewrite equation (1) as

$$\phi_p^{(2)}(r_k, \theta_k, z) = \int \int_{S_{fe}} Q^{(2)}(s) G^{(2)}(r_k, \theta_k, z; s) ds - \sum_{j=1}^{N_c} \int \int_{S_{wj}} Q^{(2)}(s) G^{(2)}(r_k, \theta_k, z; s) ds \quad (2)$$

where S_{fe} is the extended region over the whole free-surface, and S_{wj} is the water plane of the j th cylinder. This arrangement implies that we first extend the region of validity for $Q^{(2)}$ into the water planes occupied by the structures, and then subtract the contribution due to the fictitious forcing from the extended region.

We express the forcing function at a point (r_j, θ_j) inside the j th water plane as:

$$Q^{(2)}(r_j, \theta_j) = Q^{(2)}[a(\theta_j), \theta_j] \frac{r_j}{a(\theta_j)} \quad (3)$$

where $a(\theta_j)$ is the radial co-ordinate on the j th waterline at θ_j .

The major computational burden comes from the first integral on the right-hand side of equation (2). For its efficient evaluation, we expand the locked wave potential, the free-surface forcing function and the Green function into Fourier series:

$$\phi_p^{(2)}(r_k, \theta_k, z) = \sum_{n=-\infty}^{\infty} \phi_{pn}^{(2)}(r_k, z) e^{in\theta_k}, \quad Q_p^{(2)}(r, \theta) = \sum_{n=-\infty}^{\infty} Q_n^{(2)}(r) e^{in\theta} \quad (4)$$

$$G^{(2)} = \sum_{n=-\infty}^{\infty} e^{in(\theta_k - \theta)} \left\{ Z_0^{(2)}(0) Z_0^{(2)}(z) J_n(\kappa r_<) H_n(\kappa r_>) \frac{i}{4} + \frac{1}{2\pi} \sum_{q=1}^{\infty} Z_q^{(2)}(0) Z_q^{(2)}(z) I_n(\kappa_q r_<) K_n(\kappa_q r_>) \right\} \quad (5)$$

where $r_> = \max(r_k, r)$, $r_< = \min(r_k, r)$. $Z_0^{(2)}(z)$, $Z_q^{(2)}(z)$ are eigenfunctions, and $J_n(x)$, $H_n(x)$, $I_n(x)$, $K_n(x)$ are normal and modified Bessel/Hankel functions respectively.

We remark that the above-defined integrals associated with the Green function are valid in the whole fluid domain, inspite of the fact that $H_n(x)$, $I_n(x)$ possess singularities at $x \rightarrow 0$. In fact, as $x \rightarrow 0$, we use the asymptotic form of the normal and modified Bessel/Hankel functions, noting that when $r \rightarrow 0$, $Q^{(2)}(r, \theta) = rf(\theta)$; and when $r_k \rightarrow 0$, we have $Q_n^{(2)}(r) G_n^{(2)}|_{r_k \rightarrow 0} = 0$. When $r_k > 0$, except for the logarithmic singularity at $r \rightarrow r_k$, $z = 0$, no other singularity is encountered in the Green function. The logarithmic singularity was first discussed by Fenton (1978). When the field point is outside the waterplanes S_{wj} ($j = 1, 2, \dots, N_c, j \neq k$), the n th the Fourier mode of the locked wave potential can be expressed as:

$$\begin{aligned} \phi_{pn}^{(2)} &= Z_0^{(2)}(0) Z_0^{(2)}(z) \frac{\pi i}{2} \left\{ H_n(\kappa r_k) [S_1(n, r_k) - \frac{1}{2\pi} \int_0^{2\pi} Q^{(2)}(a(\theta)) e^{-in\theta} \int_0^{a(\theta)} r^2 J_n(\kappa r) dr d\theta] \right. \\ &- \phi_{p1}^{(2)}(n, r_k) + J_n(\kappa r_k) S_2(n, r_k) \left. \right\} + \sum_{q=1}^{\infty} Z_q^{(2)}(0) Z_q^{(2)}(z) \left\{ K_n(\kappa_q r_k) \left[\int_0^{r_k} Q_n^{(2)}(r) r I_n(\kappa_q r) dr \right. \right. \\ &- \frac{1}{2\pi} \int_0^{2\pi} Q^{(2)}(a(\theta)) e^{-in\theta} \int_0^{a(\theta)} r^2 I_n(\kappa_q r) dr d\theta \left. \right] \\ &- \left. \phi_{p2}^{(2)}(n, q, r_k) + I_n(\kappa_q r_k) \int_{r_k}^{\infty} Q_n^{(2)}(r) r K_n(\kappa_q r) dr \right\}, \end{aligned} \quad (6)$$

where

$$S_1(n, r_k) = \int_0^{r_k} Q_n^{(2)}(r) r J_n(\kappa r) dr;$$

$$S_2(n, r_k) = \int_{r_k}^{\infty} Q_n^{(2)}(r) r H_n(\kappa r) dr;$$

$$\begin{aligned} \phi_{p1}^{(2)}(n, r_k) &= \frac{1}{2\pi} \sum_{j \neq k}^{N_c} \sum_{m=-\infty}^{\infty} \left(\begin{array}{c} J_m(\kappa r_k) H_{n-m}(\kappa R_{jk}) \\ H_m(\kappa r_k) J_{n-m}(\kappa R_{jk}) \end{array} \right) e^{i(n-m)(\alpha_{jk} - \pi)} \\ &\int_0^{2\pi} Q^{(2)}(a(\theta_j)) e^{-in\theta_j} \int_0^{a_j(\theta_j)} r_j^2 J_n(\kappa r_j) dr_j d\theta_j, \left(\begin{array}{c} r_k < R_{jk} \\ r_k > R_{jk} \end{array} \right); \end{aligned}$$

$$\begin{aligned} \phi_{p2}^{(2)}(n, q, r_k) &= \frac{1}{2\pi} \sum_{j \neq k}^{N_c} \sum_{m=-\infty}^{\infty} \left(\begin{array}{c} I_m(\kappa r_k) K_{n-m}(\kappa R_{jk}) \\ K_m(\kappa r_k) I_{n-m}(\kappa R_{jk}) \end{array} \right) e^{i(n-m)(\alpha_{jk} - \pi)} \\ &\int_0^{2\pi} Q^{(2)}(a(\theta_j)) e^{-in\theta_j} \int_0^{a_j(\theta_j)} r_j^2 J_n(\kappa r_j) dr_j d\theta_j, \left(\begin{array}{c} r_k < R_{jk} \\ r_k > R_{jk} \end{array} \right). \end{aligned}$$

In deriving equation (6), we have used the Bessel addition theorem, R_{jk} being the horizontal distance between the j th and k th coordinate systems. A similar expression for the n th Fourier mode of the second-order locked wave component in the extended region can also be obtained.

In the case of simple geometry, e.g. for multiple bottom-seated or truncated cylinders, semi-analytical solutions for the 'free-wave' component can be obtained (Huang & Eatock Taylor 1997). Such a solution is adopted in generating the results in the next section.

2 Computation of the one-dimensional free-surface integrals

Let R_J be a large radius, such that when $r > R_J$, the local waves associated with the modified Bessel functions can be neglected, and the asymptotic forms can be used for the normal Bessel or Hankel functions. Thus integrals like $S_2(n, R_J)$ can be carried out analytically. For $r < R_J$ we can derive recurrence formulae such as the following for the free-surface integrals:

$$S_1(n, a) = 0; S_1(n, r_0 + \Delta r) = S_1(n, r_0) + \int_{r_0}^{r_0 + \Delta r} r Q_n(r) J_n(\kappa r) dr \quad (7)$$

$$S_2(n, r_0) = S_2(n, r_0 + \Delta r) + \int_{r_0}^{r_0 + \Delta r} r Q_n(r) H_n(\kappa r) dr. \quad (8)$$

Algorithms for the integrals associated with the modified Bessel functions are treated in Huang & Eatock Taylor (1997). In a small interval $[r_j, r_j + \Delta r]$, we express the forcing function $Q_n(r)$ and the Bessel/Hankel functions (or modified Bessel functions) as a quadratic function of r , and the quadrature over this interval can then be carried out analytically. A similar approach was taken by Malenica & Molin (1995), using numerical integration over a smaller interval.

3 A numerical example

As a numerical example, we consider the free-surface elevation in the vicinity of four bottom-seated cylinders of radius $a = 15.5m$, in water of depth $h = 300m$. The centre-lines of the cylinders are placed at the corners of a square of side length $L = 80m$. The incident wave is in the same direction as the x axis, which bisects two opposite sides of the square. The non-dimensional wave number is given by $ka = 0.403$; and the wave amplitude $A = 6m$.

Figures 1a and 1b illustrate respectively the linear and maximum non-linear (first order plus second order) free surface elevations around the cylinders. Figure 2 shows the contours of the non-linear free surface elevation at $t = 0$. Figure 3 plots the maximum linear and non-linear wave run-up on the up-wave and down-wave cylinders. Figure 4 presents the maximum linear and non-linear wave elevations along the x axis. From these figures, we note that the maximum wave elevation in this specific case is not at the surface of the up-wave cylinders, but is located a little distance in front of them, on the centre-line. We also see that the non-linear effect can either increase or reduce the local free surface elevation.

4 Concluding remarks

A semi-analytical procedure is proposed for evaluating the free surface integrals associated with the frequency-domain analysis of non-linear wave diffraction by multiple structures of arbitrary shape. A distinguishing characteristic of the procedure is that it is highly efficient for evaluating the non-linear potential at a large number of points. It takes only a few minutes on a Sun Workstation, for the case of a complete second-order analysis of four cylinders. With a fully numerical method, it takes over 20 hours CPU time on the same computer. This method therefore provides an efficient tool for flow visualization of non-linear wave field around multiple structures, and for undertaking third-order analyses.

This work was sponsored by EPSRC through MTD Ltd (Grant GR/L19355) and jointly funded with Den Norske Stats Oljeselskap a.s. and W.S. Atkins Consultants Ltd.

References

- [1] Fenton, J. D. (1978) Wave forces on vertical bodies of revolution. *J. Fluid Mech.* **85**, 241-255.
- [2] Malenica, S. & Molin, B. (1995) Third harmonic wave diffraction by a vertical cylinder. *J. Fluid Mech.* **302**, 203-229.
- [3] Huang, J.B. & Eatock Taylor, R. (1997) Second-order wave diffraction by a group of vertical cylinders. In preparation.

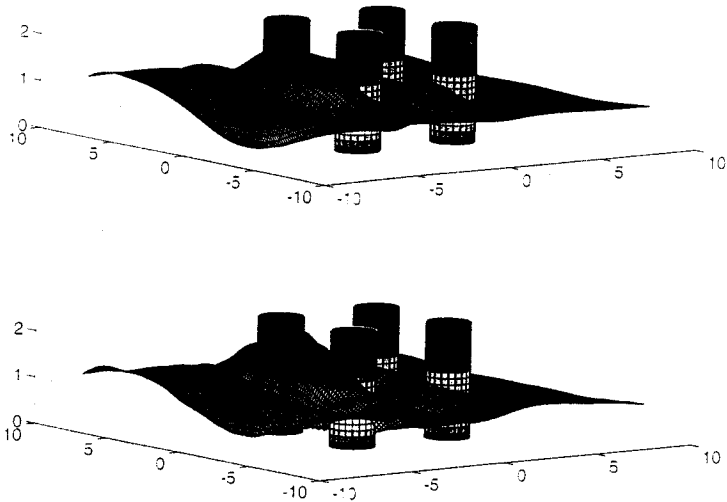


Figure 1. Isometrics of maximum free surface elevation around 4 bottom-seated cylinders: (a) first-order; (b) first-order plus second-order.

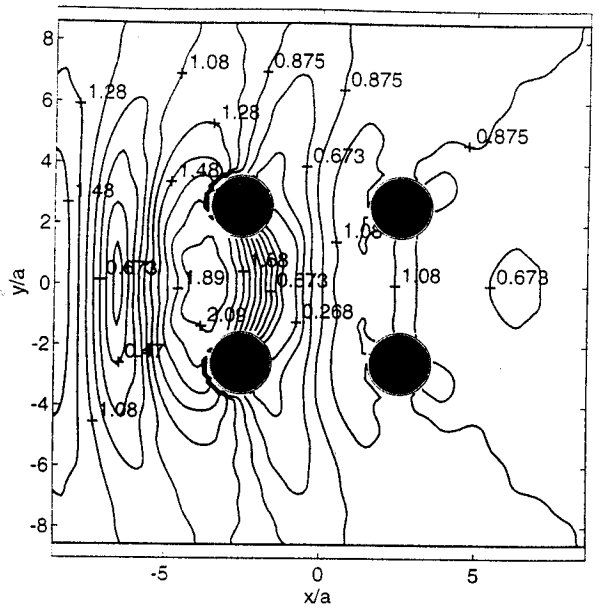


Figure 2. Contours of non-linear wave elevation at $t = 0$.

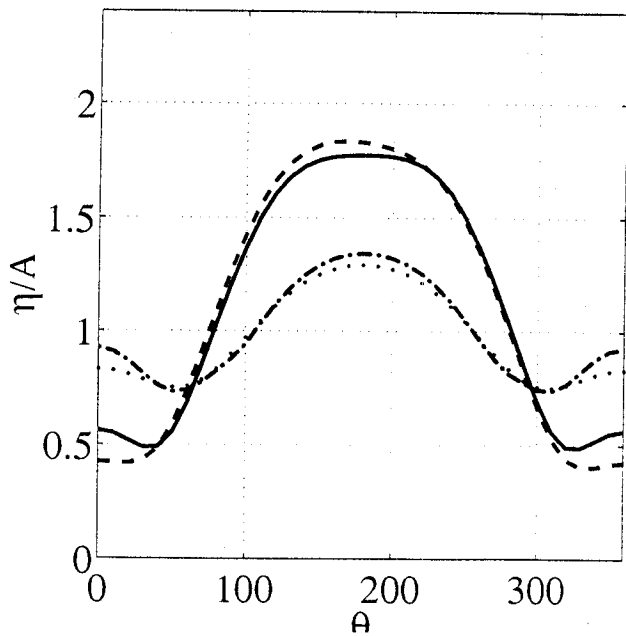


Figure 3. Maximum wave run-up around the cylinders; (—) linear, up-wave cylinder; (---) non-linear, up-wave cylinder; (.....) linear, down-wave cylinder; (-·-·-) non-linear, down-wave cylinder.

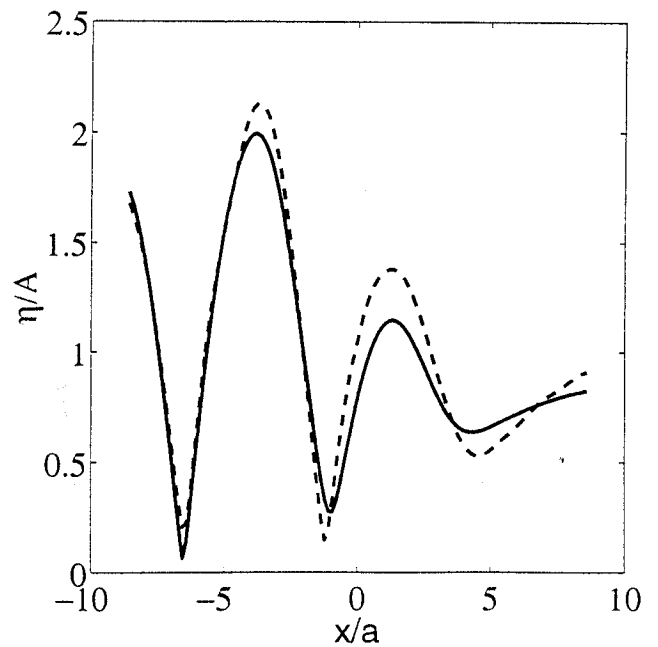


Figure 4. Maximum free surface elevation along the central line $y = 0$, (—) linear; (---) nonlinear.